ACS OMEGA

http://pubs.acs.org/journal/acsodf

Article

Properties of Multilayer Transparent Bamboo Materials

Yan Wu,* Jing Wang, Yajing Wang, and Jichun Zhou

Cite This: *ACS Omega* 2021, 6, 33747−33756

Read Online

ACCESS | Metrics & More | Article Recommendations

ABSTRACT: The objective of this study is to solve the shortcomings of the current transparent bamboo veneer with a small thickness and low light transmittance by means of lamination. The delignified bamboo templates were vacuum impregnated with an epoxy resin, and the impregnated bamboo templates were laminated with the same radial texture using the viscosity of the epoxy resin to obtain multilayer transparent bamboo (MLTB). The multilayer stacking method can greatly improve the optical and mechanical properties of transparent bamboo. The transparent bamboo with a thickness of 1.2 mm and the delignified bamboo with a volume fraction of 44.8% prepared by multilayer stacking exhibited an improved total optical transmissivity of up to 78.6%, while the highest transmittance of bamboo (0.9 mm thick) without multilayer stacking treatment was only 10.4%. Compared with the single-layer transparent bamboo with a thickness of 2.1 mm, the maximum tensile strength of the seven-layer transparent bamboo was 4 times that of the single-layer transparent bamboo. Therefore, MLTB can compensate to a certain extent for the low light transmission and poor mechanical properties of single-layer transparent bamboo. Overall, MLTB shows a richer and more layered texture, which has more esthetic value. It is a kind of natural transparent material with good light transmittance and excellent mechanical properties, which has a good development prospect as a structural material in the fields of construction, household, and electronic products.

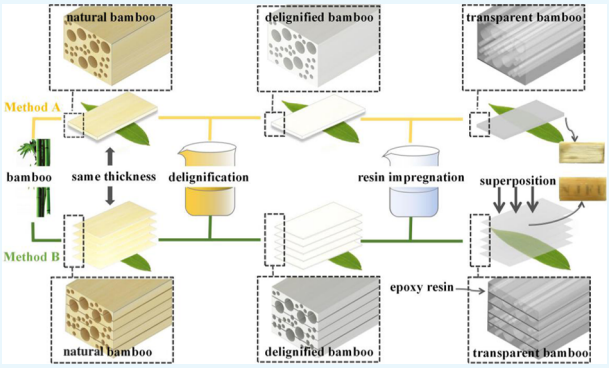

1. INTRODUCTION

Continued societal population growth and modernization will lead to a threefold increase in global resource demand.[1−3] According to the speculation of the United Nations, the amount of plastic in the ocean will exceed the amount of fish by 2050. Moreover, with the popularity of next-generation communication technologies, there is a huge demand for housing products in consumer electronics terminals such as 5G base stations, cell phones, and tablets. For a long time, almost all materials of consumer electronics shells have been petroleum-based plastic products, which have defects such as energy overconsumption, nondegradable petroleum-based plastic products, high cost, and environmental pollution.[4−6] Therefore, it is necessary to reduce the dependence on nonrenewable resources such as petroleum and focus on sustainable development and green development.[7−9] The development of green and energy-efficient materials has become a popular research topic from the perspective of sustainable development.[10] Biomass materials are widely available and renewable with low processing costs. Under the current reality of depleting nonrenewable resources, the development and utilization of new materials can effectively alleviate the severe problems of energy stress and environmental pollution if renewable biomass materials are used as the "cornerstone" of new materials instead of the traditional petrochemical-based and mineral-based materials.[11−14] In the past research, most focus has been on renewable resources and the application of natural materials in industrial production.

Biomass materials are one of the current research hotspots in the direction of materials, and the basic reason is that they have the advantages of wide sources and conform to green development. Bamboo as a renewable natural material has gradually become a research hotspot for scholars at home and abroad.[15] Bamboo is the vernacular term for perennial, giant, woody evergreen plants in the grass family Poaceae (syn. Gramineae). As a natural resource, bamboo has great potential for socioeconomic applications. The growth cycle of bamboo is only 3−5 years.[16] From the environmental point of view, comparing the oxygen released by the same volume of trees and bamboo, bamboo releases 35% more oxygen into the atmosphere than trees. Moreover, bamboo has a wide variety of species and sources around the world, with about 1500 species and 36 million hectares planted throughout Asia,

Received: September 10, 2021
Accepted: November 24, 2021
Published: December 3, 2021

America, and Africa.[17] Compared with wood, bamboo has better tensile resistance, insect resistance, abrasion resistance, water resistance, and mold resistance. The rigidity of bamboo comes mainly from the action of lignin. Since the tensile strength of bamboo is close to that of soft steel, bamboo is widely used in furniture, construction, and bridges.[18] Designers are increasingly interested in using laminated bamboo materials in buildings, such as plywood, particle board, and other laminated bamboo structural elements.[19]

Biomass materials are inherently opaque but can be modified to make them translucent so that they can replace existing optically transparent materials and be used in energy-saving materials, which has developed great potential. Currently, transparent wood (TW) as an emerging result of biomass material research has been widely noticed and studied for its many advantages of light weight, light transmission, environmental protection, and high mechanical properties.[20−25] Natural wood contains lignin and other light-absorbing components, and the porous structure of the wood will scatter visible light, resulting in the opacity of the wood, which cannot meet the demand for lighting and cannot be used as a glass material for buildings. There are two main reasons for the opacity of wood: (1) the wood contains a large amount of light-absorbing substance, that is, lignin, which accounts for 20−30% of the total weight of wood; (2) the porosity of wood is as high as 30−80%, and a large number of pores have diameters larger than the wavelength of visible light (380−780 nm), which will cause severe light scattering. Therefore, by removing the lignin in the wood, it is possible to remove the chromogenic substances while retaining the skeletal structure of the wood. The pore structure in wood mainly includes a microcapillary system (mainly formed by the dynamic connection of tiny pores with a size below 10 nm in the fine running wall) and a large capillary system (mainly composed of conduits and screens). These capillary channels are connected to each other, and so a transparent resin with a very high refractive index matching with the cellulose can be injected into it to fill the pores in the wood, thereby achieving transparency. The current method of preparing TW is to remove the lignin from wood and then fill it with a polymer whose refractive index matches that of the delignified wood template.[26−28] Methods to remove the chromogenic groups from wood include acid delignification, alkaline delignification, bioenzymatic delignification, and lignin modification.[29−31] Selection of resin is the main part of the impregnation of resin. Polymers matching the refractive index of the wood template are epoxy resins, poly(methyl methacrylate), polylactic acid, poly(vinyl alcohol), and other polymers, as well as the more environmentally friendly limonene acrylate derived from orange peel, which has been recently reported.[32]

Bamboo is an anisotropic natural composite material whose structure is mainly composed of vascular bundles (composed of thick-walled tissue, metaxylem ducts, and sieve tubes with associated cells) embedded in a wood matrix (parenchyma).[33] Bamboo has a porous layered structure similar to that of wood with the presence of many well-aligned vertical channels.[34,35] The main chemical components of bamboo are cellulose, hemicellulose, and lignin, which account for more than 90% of the total mass. The minor components are soluble polysaccharides, waxes, resins, tannins, protein, and ash.[16] Bamboo has stronger mechanical properties than wood due to the hierarchical structure and strong interactions between cellulose, hemicellulose, and lignin.[36−38] Consequently, bamboo also has the potential for use in the preparation of transparent materials. However, the high density and low porosity of bamboo make it challenging to produce transparent products.[39] The reason for this is that bamboo is denser compared to wood, and the high density inevitably reduces the permeability of the bamboo during treatment. The density of mature bamboo is usually high (about 0.65 g/cm^3), which is much higher than that of low-density wood species, such as balsa, basswood, and poplar (normally 0.1−0.4 g/cm^3) used to make TW.[39] Due to the poor permeability, bamboo requires a longer time and more chemicals to remove the lignin from it. Poor permeability affects the resin filling rate, which reduces the light transmission and mechanical properties of transparent bamboo (TB).

In response to the above challenges, this study investigated the possibility of making multilayer transparent bamboo (MLTB) with certain light transmission and high mechanical tensile strength. A simple and effective method for preparing MLTB products was successfully developed. In this work, delignified bamboo (DB) templates were prepared by a sodium chlorite method using Moso bamboo as the raw material, which was then impregnated with an epoxy resin solution to prepare MLTB by laminating multiple layers with the same grain direction. The plies were laminated in stacking sequences similar to classical plywood laminates.[40] The light transmittance, mechanical properties, and color difference of one-layer, three-layer, five-layer, and seven-layer TB were tested and compared with those of single-layer TB with the same thickness. The MLTB in this study has great potential to enrich a variety of home materials and meet the needs of the home design industry for new materials. MLTB also has good prospects in replacing glass material for buildings in the future.

2. EXPERIMENTAL SECTION

2.1. Materials. Moso bamboo (*Phyllostachys heterocycla*) (4 years old) as the original bamboo (OB) samples were collected from the Huangshan region, Anhui Province, China. It has a moisture content of 11%. Raw material specifications are shown in Table 1.

Table 1. Raw Material Specifications

species	category	thickness (mm)	length (mm)	width (mm)	density (g/cm^3)
OB-1	Moso bamboo	0.3 ± 0.05	40 ± 0.05	20 ± 0.05	0.45
OB-2	Moso bamboo	0.9 ± 0.05	40 ± 0.05	20 ± 0.05	0.45
OB-3	Moso bamboo	1.5 ± 0.05	40 ± 0.05	20 ± 0.05	0.45
OB-4	Moso bamboo	2.1 ± 0.05	40 ± 0.05	20 ± 0.05	0.45

Glacial acetic acid was purchased from Nanjing Chemical Reagent Co., Ltd. Anhydrous ethanol was purchased from Sinopharm Group Chemical Reagent Co., Ltd. Electric thermostatic blast drying oven (model DHG-9423A) was purchased from Shanghai Jinghong Experimental Equipment Co., Ltd. Electronic balance (model UTP-313) was purchased from Shanghai Huachao Electric Co., Jintan City Guowang Experimental Instrument Factory. E51 epoxy resin, a low-molecular-weight liquid bisphenol A epoxy resin, was obtained from Kunshan Jiulimei Electronic Materials Co., Ltd. Its epoxy value (equivalent/100 g) is 0.48−0.54 and viscosity (MPAS/

https://doi.org/10.1021/acsomega.1c05014
ACS Omega 2021, 6, 33747−33756

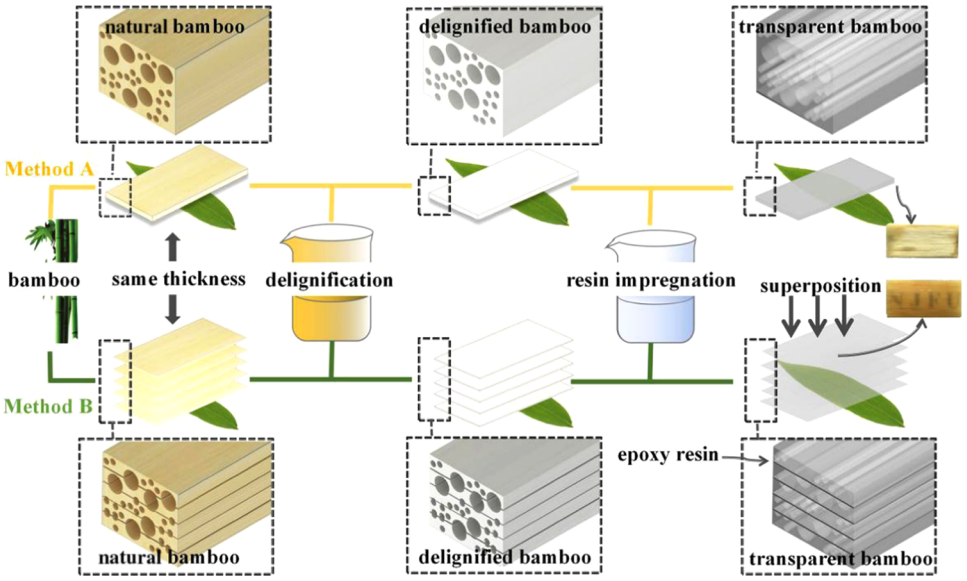

Figure 1. Schematic diagram of different processing routes from the natural bamboo to the TB.

25 °C) is 11 000−14 000. B210 epoxy resin curing agent, a new type of amine greenhouse curing agent modified by polyether amine, was purchased from Kunshan Jiulimei Electronic Materials Co., Ltd.; its viscosity (MPAS/25°C) is 200−300, the relative density at 20 °C is 1.03−1.08 g/cm^3, and the amine value (KOH mg/g) is 300−400.

2.2. Experimental Methods. As shown in Figure 1, different processing methods can be used to prepare TB with the same thickness. Method A is to process a whole piece of bamboo directly. Method B is to cut a whole piece of bamboo into thin slices, treat the thin slices, and then laminate the impregnated bamboo samples in the same radial grain during resin impregnation. To facilitate the description of the characterization of the samples, this study numbered the sample types that would appear in the test. Specifically, "A" and "B" refer to the transparent bamboo prepared by method A and method B, respectively.

2.2.1. Preprocessing. The OB samples were placed in the oven and dried at 100−110 °C for 6−10 h. The absolutely dried OB samples were taken out for the next experiment.

2.2.2. Preparation of the Delignified Bamboo Templates. A sodium chlorite aqueous solution with a concentration of 3.5 wt % was prepared, stirred well, and then glacial acetic acid was added dropwise to obtain a solution of pH 4.6. The OB samples were placed in the solution and heated by immersion in a digital triple-use thermostat for 2−3 h. Then, the samples were rinsed with distilled water and stored in anhydrous ethanol to obtain the delignified bamboo (DB) templates. In this step, DB templates with a thickness of 0.3 mm (DB-1), DB templates with a thickness of 0.9 mm (DB-2), DB templates with a thickness of 1.5 mm (DB-3), and DB templates with a thickness of 2.1 mm (DB-4) were obtained.

2.2.3. Preparation of the Transparent Bamboo. With the above treatment, delignified bamboo is still opaque because light is scattered in the lumen at the interface between the cell wall and air and at the interface between cellulose nanofibers and air in the cell wall. To obtain high light transmittance, delignified bamboo strips were soaked in an epoxy resin with a refractive index of 1.52. The epoxy resin impregnation solution was prepared at an epoxy resin-to-hardener weight ratio of 2:1. The DB templates were impregnated with the epoxy resin solution and vacuum impregnated for 15−30 min. Finally, the impregnated samples were placed in two pieces of silica gel to cure at room temperature at 20−40 °C. The TB samples were obtained after 12−20 h of sealing and curing. The obtained samples were labeled as TB-1, TB-2A, TB-3A, and TB-4A, which referred to the single-layer TB with thicknesses of 0.3, 0.9, 1.5, and 2.1 mm, respectively.

2.2.4. Preparation of the Multilayer Transparent Bamboo. The samples that were vacuum impregnated with the epoxy resin impregnation solution for 25−30 min were taken out, and then they were laminated with the same radial texture. Then, the samples were placed in two pieces of silica gel and fixed with clamps, and then a certain pressure was applied and cured at room temperature of 20−40 °C. Finally, the MLTB samples were obtained after 12−20 h of sealing and curing. TB-2B refers to the three-layer TB prepared by method B with a thickness of 1.2 mm. TB-3B refers to the five-layer TB prepared by method B with a thickness of 2.3 mm. TB-4B refers to the seven-layer TB prepared by method B with a thickness of 2.9 mm.

3. CHARACTERIZATION

3.1. Fourier Transform Infrared Spectroscopy-Attenuated Total Reflection Characterization. The samples were taken and ground into a powder with potassium bromide; the powder was pressed into a transparent sheet under a press, and then the pressed transparent sheet was tested in a Fourier transform infrared spectrometer (VERTEX 80V, Bruker Spectroscopy Instruments) to analyze the changes in the chemical bonds of the samples.

3.2. Scanning Electron Microscopy Measurements. The samples were cut perpendicular to the bamboo fiber direction using an ultrathin sectioning machine and then vacuum plated, and the cross-sectional morphology of the samples was observed at 150× and 600× magnification using a scanning electron microscope (FEI Quanta 200, FEI Inc.) with secondary electron signal imaging.

3.3. UV Transmittance Measurements. The UV transmittance measurements of OB, MLTB, and single-layer TB

https://doi.org/10.1021/acsomega.1c05014
ACS Omega 2021, 6, 33747−33756

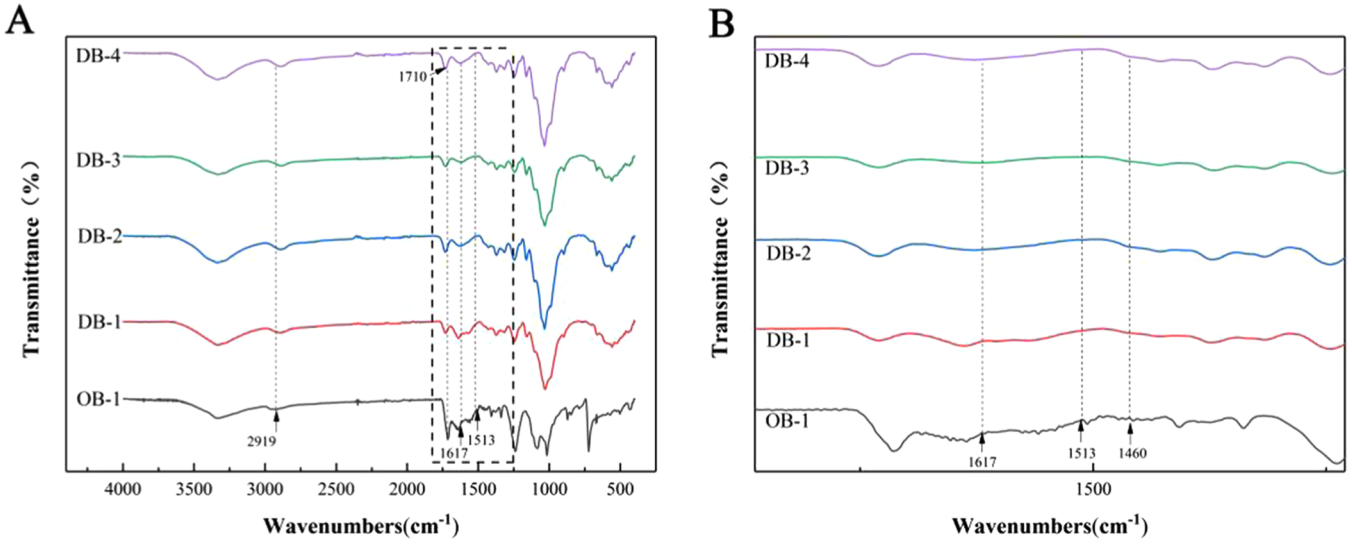

Figure 2. FTIR curves of the samples before and after delignification treatment ((B) is the enlarged picture of the dotted box in (A)).

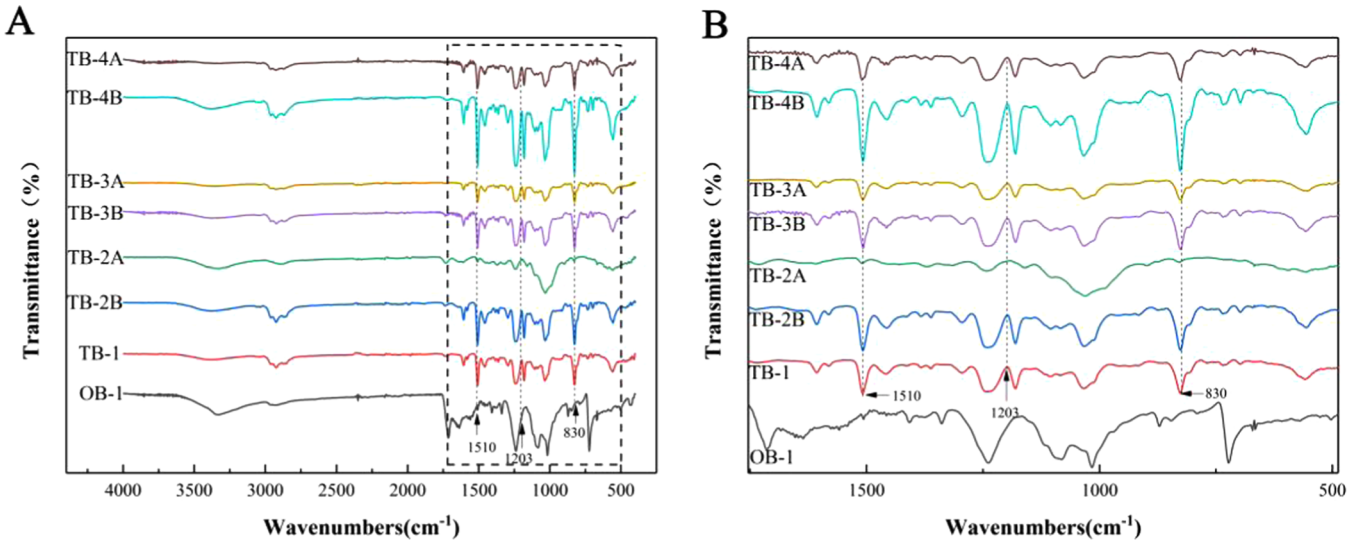

Figure 3. FTIR curves of the samples before and after transparency treatment ((B) is the enlarged picture of the dotted box in (A)).

samples were performed at 350−800 nm using a Lambda 950 UV−visible spectrometer (PerkinElmer).

3.4. Haze Measurements. The haze measurements of OB, MLTB, and single-layer TB samples were performed at 350−800 nm using a Lambda 950 UV−visible spectrometer (PerkinElmer). The haze value is calculated according to eq 1.

$$\text{haze} = \left(\frac{T_1}{T_2} - \frac{T_3}{T_4}\right) \times 100 \tag{1}$$

where T_1 represents the beam of the incoming light, T_2 represents the beam of the transmitted light, T_3 represents the beam of the diffused light from the system, and T_4 represents the beam of the diffused light from the system and sample.

3.5. Volume Fraction of Delignified Bamboo. The volume fraction of delignified bamboo in the transparent bamboo was calculated according to eqs 2 and 3.[41]

$$V_f = \frac{W_f \times \rho_c}{\rho_f} \tag{2}$$

$$\rho_c = \frac{1}{\frac{W_f}{\rho_f} + \frac{W_m}{\rho_m}} \tag{3}$$

where V_f is the volume fraction of the delignified bamboo in the transparent bamboo, ρ_c is the density of the composite, ρ_f is the density of the delignified bamboo, ρ_m is the density of the epoxy (1.08 g/cm^3), W_m is the weight fraction of the epoxy, and W_f is the weight fraction of the delignified bamboo.

3.6. Color Difference Measurements. The color analysis of each sample was performed using a PANTONE color detector (model: RM200, Ashley Co., Ltd.). The test was repeated three times for each sample, and the average value was obtained; the samples were analyzed using the L^*a^*b homogeneous color space system. L^* denotes luminosity, where a completely white object is regarded as 100 and a completely black object is regarded as 0. The larger the value, the higher the luminosity. a^* denotes redness, where a larger positive value indicates a more reddish color and a larger negative value indicates a more greenish color. b^* denotes yellowness, where a larger positive value indicates a more

https://doi.org/10.1021/acsomega.1c05014
ACS Omega 2021, 6, 33747−33756

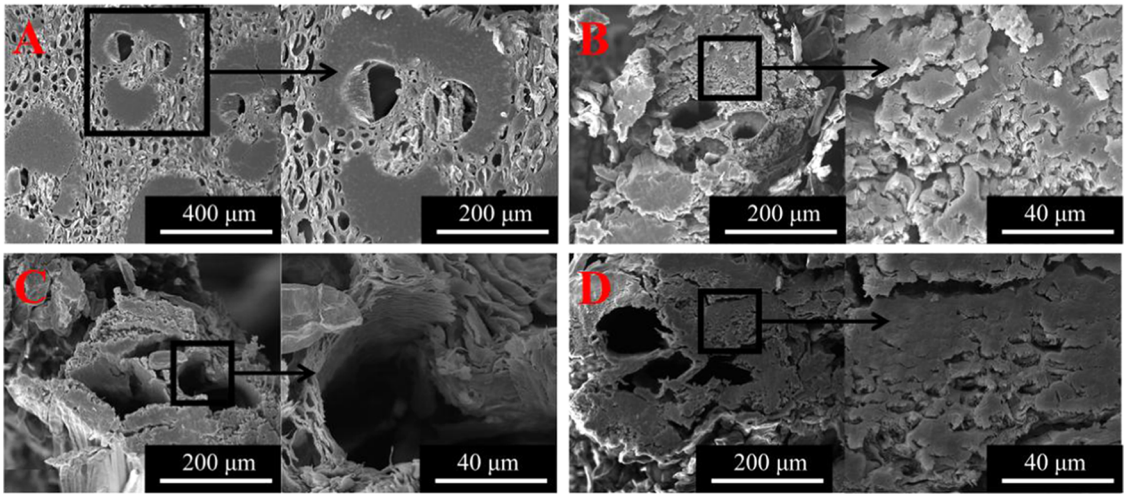

Figure 4. SEM images of OB and DB of different thicknesses: (A) OB; (B) DB-2; (C) DB-3; and (D) DB-4.

yellowish color and a larger negative value indicates a more bluish color.

3.7. Mechanical Performance Measurements. The mechanical performance measurements of OB, MLTB, and single-layer TB samples were performed using an AG-IC precision electronic mechanical testing machine (Shimadzu Manufacturing, Japan). Three parallel sets of each sample were taken and tested to obtain the average value. The jig of the testing machine stretched the samples along the direction of the grain until rupture, setting the stretching rate at 5 mm/min and the maximum load force at 10 000 N. Particularly, the clamp holding the upper part of the sample keeps moving, while the clamp holding the lower part of the sample remains stationary. According to the equation of $P = F/S$, the maximum tensile strength of the specimens can be calculated:[42−44] S refers to the area subjected to the force, F refers to the total force on the area, and P refers to the pressure.

4. RESULTS AND DISCUSSION

4.1. Fourier Transform Infrared Spectroscopy-Attenuated Total Reflection Analysis. As shown in Figure 2, the characteristic absorption peaks of OB included the stretching vibration of the C−H group at 2919 cm^{-1}, the stretching vibration of the acetyl group in hemicellulose at 1710 cm^{-1}, the stretching vibration of the aromatic ring group in lignin at 1617 cm^{-1}, the stretching vibration of the C═O group at 1513 cm^{-1}, the stretching vibration of the C═O group at 1460 cm^{-1}, and symmetric stretching vibrations and the stretching vibration of the O−H group in cellulose at 3334 cm^{-1}.[45,46]

The curves of DB-1, DB-2, DB-3, and DB-4 are of the delignified bamboo. It can be seen that the absorption peaks at 1617, 1513, and 1460 cm^{-1} disappeared in the delignified samples, which means that the lignin was removed from the bamboo in a large amount after the delignification process. And overall, no new functional groups were added.

From Figure 3, it can be seen that the absorption peaks of the epoxy resin newly appear in the FTIR spectrum of TB samples, including the peak at 1510 cm^{-1} due to the −C═C− bending vibration of the para-substituted benzene ring, antisymmetric stretching vibration at 1203 cm^{-1} due to an aliphatic−aromatic ether C−O−C, and out-of-plane deformation of the para-substituted benzene ring ═ CH at 830 cm^{-1}.[47] This result is consistent with the FTIR test study of transparent bamboo reported by Wu et al.[48] It indicated that the internal lignin groups were almost removed from the samples after delignification treatment. The transparent sample contained not only the molecular groups of the bamboo itself but also the molecular groups of the epoxy resin, indicating that the resin successfully penetrated into the bamboo.

4.2. Scanning Electron Microscopy Analysis. It can be seen from Figure 4 that vascular tissue and parenchyma cells are present in the cross-section of OB. Features such as invaginations in the cells can be clearly seen. The destruction of vascular tissue and deformation of parenchyma cells after delignification treatment are shown in Figure 4. It can be observed that the cell walls of the pretreated bamboo show more microporous structures, which was mainly caused by the partial removal of extractives, hemicellulose, and lignin components, from the cell walls. It can be seen from Table 2 that the greater the thickness, the higher the weight loss rate of bamboo, the longer the delignification treatment time, but the more obvious the damage of the sample after delignification. In general, micropores and nanopores are formed in the cell wall after lignin removal, and the resulting micropores could facilitate the penetration of epoxy resin into the bamboo template. However, the porous structure also caused large light scattering in the visible region, and such microstructures could lead to increased light scattering within the cell wall, affecting transmittance and haze.

Table 2. Weight Before and After Delignification of Raw Bamboo of Different Thicknesses

species	thickness (mm)	weight before delignification (g)	weight after delignification (g)	weight differential (g)
OB-1	0.3 ± 0.05	0.108	0.080	0.028
OB-2	0.9 ± 0.05	0.450	0.323	0.127
OB-3	1.5 ± 0.05	0.688	0.389	0.299
OB-4	2.1 ± 0.05	0.892	0.492	0.400

As shown in Figure 5, the epoxy resin was successfully impregnated into TB-1; the surface of TB-1 was homogeneous with almost no debonding gaps,[49] and hence TB-1 showed better light transmission. Nevertheless, the other thicknesses of single-layer TB samples showed cell deformation, vascular

https://doi.org/10.1021/acsomega.1c05014
ACS Omega 2021, 6, 33747−33756

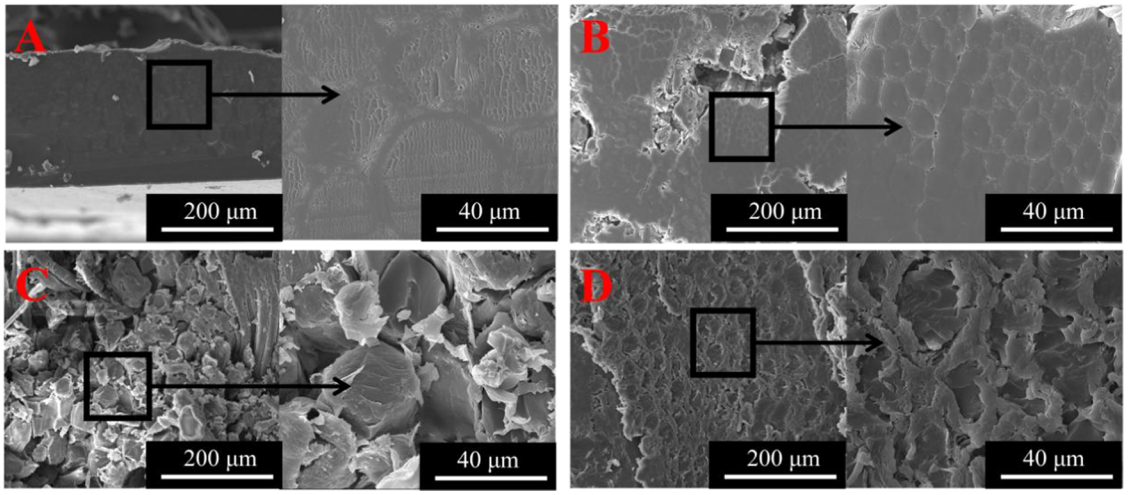

Figure 5. SEM images of the single-layer TB: (A) TB-1; (B) TB-2A; (C) TB-3A; and (D) TB-4A.

bundle tissue destruction, and increased gaps, which indicated that the epoxy resin failed to completely bond with the thicker monolayer DB templates, and the larger the interfacial cracks, the more likely light scattering would occur, thus reducing the transparency.

Figure 6 shows the surface of the MLTB covered with epoxy resin in a uniform state, indicating that the epoxy resin was successfully impregnated and cured in the multilayer samples. However, there was a debonding gap between the cell wall of the multilayer TB and the epoxy resin. The gap becomes obvious as the thickness increases. For example, compared with TB-2B, the gap between the cell wall of TB-3B and the epoxy resin is larger, which indicates that the epoxy resin is not fully infiltrated into TB-3B, which will make the light transmittance of TB-3B less than that of TB-2B. In addition to the debonding gap, the presence of voids will endow the interface with a higher refractive index contrast, which would increase the light scattering and reduce light transmission. Therefore, the light transmission of multilayer TB decreases as the thickness increases. However, even though there were gaps between layers in MLTB, the light transmission rate was still higher than that of the single-layer TB under the same thickness condition. Compared with TB of the same thickness, MLTB has fewer internal cracks, and the combination of epoxy resin and cell wall is better. All in all, the multilayer stacking method could effectively improve the light transmission of TB.

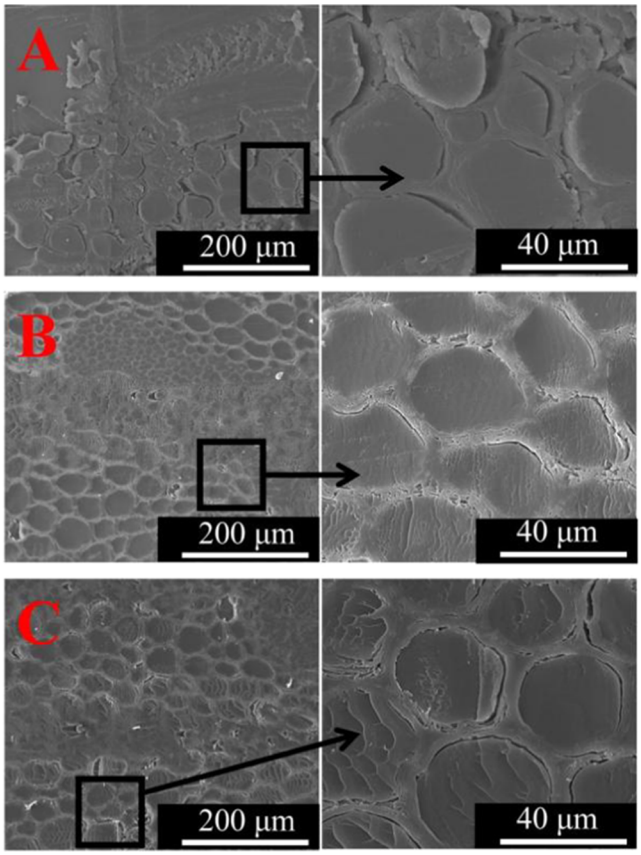

Figure 6. SEM images of MLTB: (A) TB-2B; (B) TB-3B; and (C) TB-4B.

4.3. Optical Performance Analysis. As shown in Figure 7A and Table 2, the light transmittance of the OB samples was negligible. TB-1 (0.3 mm thick) exhibited a transmittance of 92.4% and a haze of 43.5% at the 800 nm wavelength (Figure 7A,C). Wu et al.[48] reported that the maximum transmittance of the single-layer transparent wood (TW) with a thickness of 0.5 mm was only 4%. The higher the thickness, the longer the distance the light travels inside the TW and the lesser the light transmitted.[50] The light transmittance of TB-2B, TB-3B, and TB-4B gradually decreased. The reason is that light is scattered and absorbed inside the samples. The highest light transmission rate was 78.6% for TB-2B (1.2 mm thick), 67.1% for TB-3B (2.3 mm thick), and 53.7% for TB-4B (2.9 mm thick). As reported, the maximum transmittance of the three-layer TW with a thickness of 1.5 mm was about 1.2% and that of the five-layer TW with a thickness of 2.5 mm was about 0.45%.[48] Compared with the single-layer TB, the light transmittance of the MLTB was higher than that of the single-layer one, i.e., TB-2B > TB-2A, TB-3B > TB-3A, and TB-4B > TB-4A, and the longer the wavelength, the higher the light transmittance. After superposition processing, the haze of the MLTB increased. TB-2B (1.2 mm thick) exhibited a haze of 70% at the 800 nm wavelength. As the thickness increased, the haze of MLTB also increased. Under the condition of the same thickness, the haze of MLTB was lower than that of the single-layer TB.

Figure 7D–I shows the macroscopic observation diagram of the MLTB and the single-layer TB. Compared with the OB

https://doi.org/10.1021/acsomega.1c05014
ACS Omega 2021, 6, 33747−33756

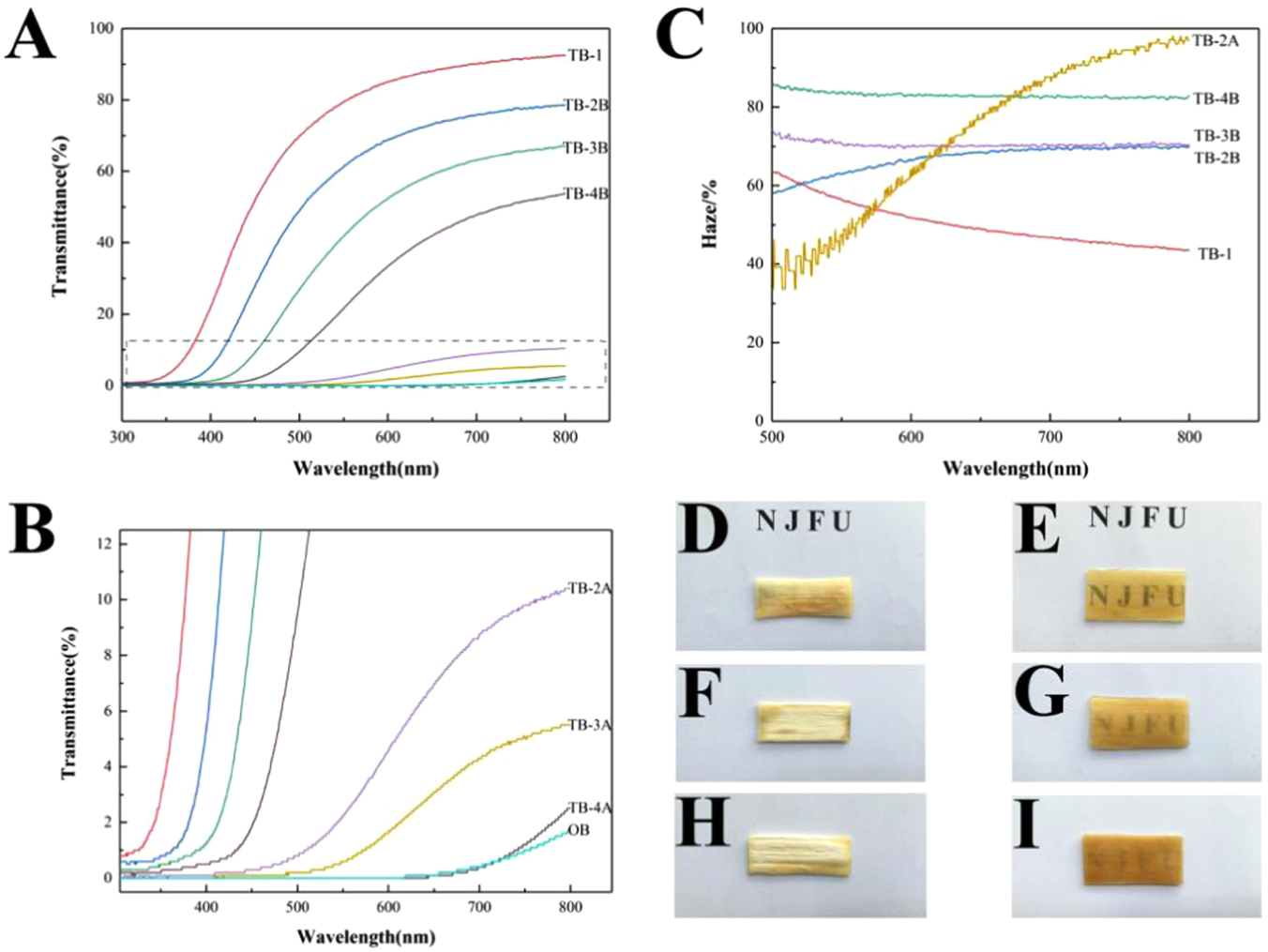

Figure 7. (A, B) Lighttransmission of OB and TB (B is the enlarged picture of the dotted box in A). (C) Optical haze curves of MLTB and single-layer TB. (A, B) Light transmission of OB and TB (B is the enlarged picture of the dotted box in A; C is the enlarged picture of the dotted box in (B)). (C) Optical haze curves of MLTB and single-layer TB. (D) Macroscopic observation diagram of TB-2A. (E) Macroscopic observation diagram of TB-2B. (F) Macroscopic observation diagram of TB-3A. (G) Macroscopic observation diagram of TB-3B. (H) Macroscopic observation diagram of TB-4A. (I) Macroscopic observation diagram of TB-4B.

samples, the light transmittance of TB was improved, and the light transmittance of MLTB gradually decreased with the stacking of layers. However, the light transmittance of MLTB was much higher than that of the single-layer TB. Therefore, the use of multilayer lamination can effectively improve the light transmittance of transparent bamboo under the same thickness conditions.

Table 3 shows that the optical performance of TB depends on the volume fraction of bamboo in TB. When the volume fraction of delignified bamboo was 33.8%, the light transmittance of the 0.3 mm thick TB reached the maximum (92.4%) and the haze was the lowest (43.5%). For example, the volume fraction of the delignified bamboo in TB-2A was 72.1%, but the volume fraction of the delignified bamboo in TB-2B prepared by method B was reduced to 44.8%. Compared with the light transmittance of TB-2A (10.4%), the light transmittance of TB-2B (78.6%) was significantly improved. When the volume fraction of delignified bamboo in TB was smaller, the light transmittance of TB was higher and the haze was lower. Therefore, the method of preparing transparent bamboo by multilayer stacking can reduce the volume fraction of delignified bamboo in TB, thereby improving the optical performance of MLTB.

Table 3. Optical Properties and Volume Fraction of Delignified Bamboo

species	thickness (mm)	highest light transmission (%)	haze (%)	volume fraction of delignified bamboo (%)
TB-1	0.3 ± 0.05	92.4	43.5	33.8
TB-2A	0.9 ± 0.05	10.4	97.02	72.1
TB-2B	1.2 ± 0.05	78.6	70.0	44.8
TB-3A	1.5 ± 0.05	5.5	~100	75.9
TB-3B	2.3 ± 0.05	67.1	70.55	35.8
TB-4A	2.1 ± 0.05	1.7	~100	76.5
TB-4B	2.9 ± 0.05	53.7	82.95	41.7

4.4. Color Difference Analysis. Bamboo color is an important factor influencing consumer choice, and bamboo has excellent decorative features. Although cellulose and hemicellulose are optically colorless, lignin is one of the main causes of bamboo coloration. The higher the lignin content, the larger the *b* value.[51−53] Conventional bamboo is yellowish in color and shows an amberlike yellow translucency with transparent

https://doi.org/10.1021/acsomega.1c05014
ACS Omega 2021, 6, 33747−33756

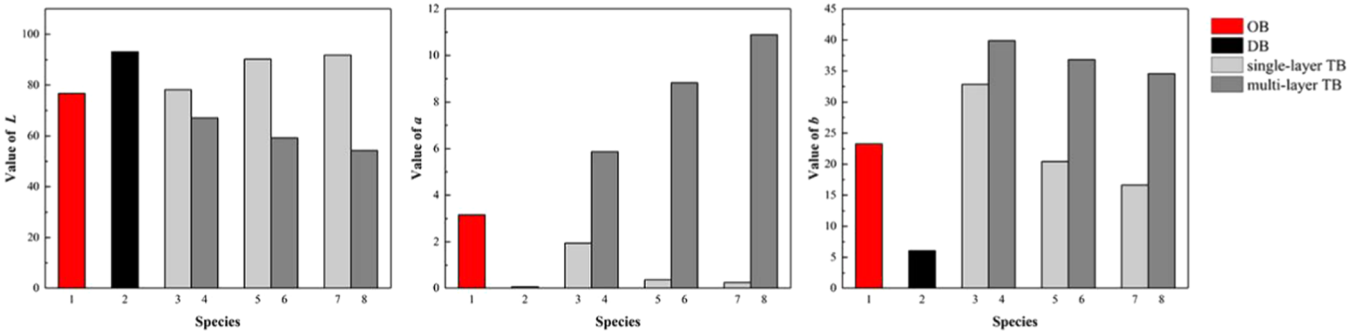

Figure 8. $L^*a^*b^*$ values of OB, DB, single-layer TB, and MLTB (1, OB; 2, DB; 3, TB-2A; 4, TB-2B; 5, TB-3A; 6, TB-3B; 7, TB-4A; and 8, TB-4B).

treatment. As seen in Figure 8, the OB chromaticity tended to be yellow-green. Compared with OB, the brightness of DB increased and the yellow color of DB was reflected in the b value in different degrees. This can be attributed to the presence of lignin residue in bamboo after delignification. The *b* value is different with different lignin contents. After the transparency treatment, the *b* value of both MLTB and single-layer TB gradually decreased with increasing thickness. However, under the same thickness condition, the *b* value of MLTB was higher than that of single-layer TB.

The *L* values of the single-layer TB prepared by method A were higher than those of the MLTB prepared by method B at the same thickness, indicating that the single-layer TB was brighter and more inclined to white. However, the *a* and *b* values of single-layer TB were lower than those of MLTB with the same thickness, indicating that the MLTB tended to be more red and yellow. The appearance of TB-2A, TB-3A, and TB-4A was white and yellow was not obvious. The reason is that the epoxy resin could not be completely impregnated into bamboo templates with the increasing thickness. This is consistent with the results of the study in Figure 7. TB-2B, TB-3B, and TB-4B were clear amber in appearance. As a result, compared with the single-layer TB with white color, the MLTB presented a unique texture and color that was very innovative and beautiful (Figure 7E,G,I), which showed that the MLTB had great potential in the field of functional decorative materials.

4.5. Mechanical Property Analysis. As seen in Figure 9, the maximum tensile strength value of DB was significantly lower than that of OB (19.19 and 24.64 MPa, respectively). The reason for this is that lignin is one of the components that make up the plant cell wall and has the effect of keeping the cells connected and enhancing the mechanical properties, while after delignification, the bamboo cell wall was destroyed, and therefore, the mechanical properties were also significantly reduced. After the transparency treatment, the maximum tensile strength values of TB were significantly increased up to 47.10 MPa. The maximum tensile strength of epoxy resin is 15.69 MPa, which is lower than that of OB. The tensile strength of the interface between the two layers is lower than that of OB. The bamboo fiber template had an enhancement function, and therefore, its tensile strength was higher than that of the epoxy resin. As the number of layers of transparent bamboo increased, the epoxy resin in the adjacent layers also increased, and the difference between the maximum tensile strength values and those of the OB gradually increased.

The maximum tensile strength value of the multilayer MLTB was 61.89 MPa, and that of the single-layer TB was

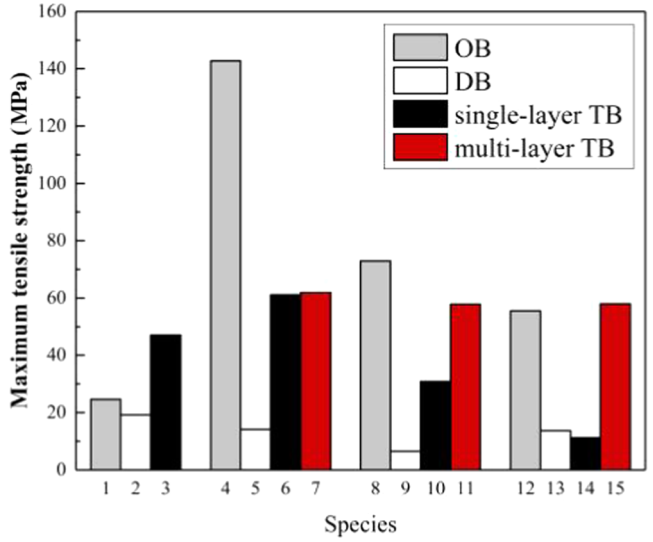

Figure 9. Maximum tensile strength of OB, DB, and TB (1, OB-1; 2, DB-1; 3, TB-1; 4, OB-2; 5, DB-2; 6, TB-2A; 7, TB-2B; 8, OB-3; 9, DB-3; 10, TB-3A; 11, TB-3B; 12, OB-4; 13, DB-4; 14, TB-4A; 15, TB-4B).

61.15 MPa. As reported, the maximum tensile strength of the single-layer TW with a thickness of 0.5 mm was 10 MPa, and that of the three-layer TW with a thickness of 1.5 mm could reach about 25 MPa.[48] This showed that TB had better tensile properties than TW with the same thickness. It could be concluded from Figure 9 that the maximum tensile strength of the MLTB was higher than that of the single-layered TB with the same thickness. For example, the maximum tensile strength of TB-3B was higher than that of TB-3A. The same is true between TB-4A and TB-4B. The reason for this is that the tensile strength of the TB is related to interfacial compatibility. The higher the interfacial compatibility, the higher the tensile strength of the TB. As the bamboo template is thicker, it is not only difficult to remove lignin completely but it is also difficult for the epoxy resin to penetrate into the DB templates. As seen in Figure 5, the deformation of single-layer TB cells and the destruction of vascular bundle tissue were severe, and the interface crack between the epoxy resin and monolayer DB template was large. However, as seen in Figure 6, the lignin could be better removed using thinner bamboo as raw materials, and thus the epoxy resin was easier to be impregnated, the surface of MLTB was smoother, and the interface compatibility between the epoxy resin and DB template was better. The multilayer TB was laminated with the

https://doi.org/10.1021/acsomega.1c05014
ACS Omega 2021, 6, 33747−33756

thin bamboo, which is more uniformly impregnated with epoxy resin and has a smoother interface, reflecting the compatibility of the resin with the DB templates. However, the thicker single-layer transparent TB was directly impregnated with resin. Penetration of resin into the bamboo cells was difficult. Moreover, the impregnation effect was not uniform and the interface was incompatible with larger gaps, which greatly affected the tensile strength values of the single-layer transparent bamboo. Meanwhile, in this test, the difference between the maximum tensile strength value of the MLTB and that of the single-layer TB gradually increased with the increasing thickness of bamboo, indicating that the mechanical advantage of the multilayer transparent bamboo became more obvious with the greater thickness. In general, the tensile strength of the MLTB was better than that of the single-layer TB under the same thickness condition. The tensile strength of MLTB was greater, and it was more suitable as a structural material for applications in household, electronics, and construction.

5. CONCLUSIONS

In summary, MLTB with high mechanical strength, optical properties, and appearance was developed by removing lignin from bamboo veneer and impregnating epoxy resin into bamboo cellulose templates. Compared with single-layer TB and MLTB, due to fewer interfacial cracks and more uniform resin coverage in MLTB, the light transmission of MLTB was higher than that of single-layer TB with the same thickness. The transparent amber appearance of MLTB exhibited a unique texture and color, which indicates that it has great potential in the field of functional decorative materials. In addition, the tensile strength of MLTB was higher than that of the single-layer TB. Transparent bamboo can improve the water absorption of bamboo to a certain extent and can effectively reduce the water expansion and drying shrinkage of bamboo due to moisture. Because of the combination of good optical properties, excellent mechanical strength, unique esthetic value, and fast renewable raw materials, the MLTB in this study has great potential to enrich a variety of household materials and meet the needs of the home design industry for new materials. Multilayer transparent bamboo also has a good prospect in replacing glass material for buildings in the future. Combined with the current process conditions, transparent bamboo is limited by the thickness direction. Therefore, multilayer transparent bamboo can be prepared by a lamination method so as to obtain materials with a large thickness, high light transmittance, and excellent mechanical properties. Multilayer transparent bamboo has a good development prospect in the future.

AUTHOR INFORMATION

Corresponding Author

Yan Wu − *College of Furnishings and Industrial Design, Nanjing Forestry University, Nanjing 210037, China;* orcid.org/0000-0003-3406-3627; Email: wuyan@njfu.edu.cn

Authors

Jing Wang − *College of Furnishings and Industrial Design, Nanjing Forestry University, Nanjing 210037, China*

Yajing Wang − *College of Furnishings and Industrial Design, Nanjing Forestry University, Nanjing 210037, China;* orcid.org/0000-0002-6766-2549

Jichun Zhou − *College of Furnishings and Industrial Design, Nanjing Forestry University, Nanjing 210037, China;* orcid.org/0000-0002-3116-9349

Complete contact information is available at: https://pubs.acs.org/10.1021/acsomega.1c05014

Funding

This work was supported by the National Natural Science Foundation of China [Grant Numbers 32071687 and 32001382], the Special Scientific Research Fund of Construction of High-Level Teachers Project of Beijing Institute of Fashion Technology (Grant Number BIFTQG201805), and the Project of Science and Technology Plan of Beijing Municipal Education Commission (Grant Number KM202010012001).

Notes

The authors declare no competing financial interest.

ACKNOWLEDGMENTS

The authors thank the teacher of the Modern Analysis Center of Nanjing Forestry University for their help in instrument testing.

REFERENCES

(1) Mohanty, A. K.; Vivekanandhan, S.; Pin, J. M.; Misra, M. Composites from renewable and sustainable resources: challenges and innovations. *Science* **2018**, *362*, 536−542.

(2) Liu, Y.; Hu, J.; Wu, Z. Fabrication of coatings with structural color on a wood surface. *Coatings* **2020**, *10*, No. 32.

(3) Xia, C.; Su, S.; Sonne, C. Seize China's momentum to protect pangolins. *Science* **2021**, *371*, 1214.

(4) Chen, Z.; Gao, H.; Li, W.; Li, S.; Liu, S.; Li, J. Advances in research on biomass-based photographic materials. *J. For. Eng.* **2020**, *5*, 1−12.

(5) Zhao, Z.; Wu, D.; Huang, C.; Zhang, M.; Umemura, K.; Yong, Q. Utilization of enzymatic hydrolysate from corn stover as a precursor to synthesize an eco-friendly adhesive for plywood II: investigation of appropriate manufacturing conditions, curing behavior, and adhesion mechanism. *J. Wood Sci.* **2020**, *66*, No. 85.

(6) Zhao, Z.; Huang, C.; Wu, D.; Chen, Z.; Zhu, N.; Gui, C.; Zhang, M.; Umemura, K.; Yong, Q. Utilization of enzymatic hydrolysate from corn stover as a precursor to synthesize an eco-friendly plywood adhesive. *Ind. Crops Prod.* **2020**, *152*, No. 112501.

(7) Sun, S.; Zhao, Z. Influence of acid on the curing process of tannin-sucrose adhesives. *BioResources* **2018**, *13*, 7683−7697.

(8) Xia, C.; Lam, S.; Sonne, C. Ban unsustainable mink production. *Science* **2020**, *370*, 539.

(9) Hu, W.; Guan, H. A finite element model of semi-rigid mortise-and tenon joint considering glue line and friction coefficient. *J. Wood Sci.* **2019**, *65*, No. 14.

(10) Sonne, C.; Xia, C.; Su, S. Ancient oaks of Europe are archives-protect them. *Nature* **2021**, *594*, 495.

(11) Gurunathan, T.; Mohanty, S.; Nayak, S. K. A review of the recent developments in biocomposites based on natural fibres and their application perspectives. *Composites, Part A* **2015**, *77*, 1−25.

(12) Li, T.; Song, J.; Zhao, X.; Yang, Z.; Pastel, G.; Xu, S.; Jia, C.; Dai, J.; Chen, C.; Gong, A.; et al. Anisotropic, lightweight, strong, and super thermally insulating nanowood with naturally aligned nano-cellulose. *Sci. Adv.* **2018**, *4*, No. eaar3724.

(13) Xu, W.; Fang, X.; Han, J.; Wu, Z.; Zhang, J. Effect of Coating Thinckness on Sound Absorption Property of Four Wood Species Commonly Used for Piano Soundboards. *Wood Fiber Sci.* **2020**, *52*, 28−43.

(14) Liu, H.; Zhang, J.; Jiang, W.; Cai, Y. Characteristics of commercial-scale radio-frequency/vacuum (RF/V) drying for hard-wood lumber. *BioResources* **2019**, *14*, 6923−6935.

(15) Sun, X.; He, M.; Li, Z. Novel engineered wood and bamboo composites for structural applications: state-of-art of manufacturing technology and mechanical performance evaluation. *Constr. Build. Mater.* **2020**, *249*, No. 118751.
(16) Wu, Y.; Wang, Y.; Yang, F.; Wang, J.; Wang, X. Study on the properties of transparent bamboo prepared by epoxy resin impregnation. *Polymers* **2020**, *12*, No. 863.
(17) Nayak, L.; Mishra, S. P. Prospect of bamboo as a renewable textile fiber, historical overview, labeling, controversies and regulation. *Fashion Text.* **2016**, *3*, No. 2.
(18) Li, Z.; Chen, C.; Mi, R.; Gan, W.; Hu, L. A strong, tough, and scalable structural material from fast-rowing bamboo. *Adv. Mater.* **2020**, *32*, No. 1906308.
(19) Montanari, C.; Ogawa, Y.; Olsén, P.; Berglund, L. High performance, fully bio-based, and optically transparent wood biocomposites. *Adv. Sci.* **2021**, *8*, No. 2100559.
(20) Fink, S. Transparent wood − a new approach in the functional study of wood structure. *Holzforschung* **1992**, *46*, 403−408.
(21) Iwamoto, S.; Nakagaito, A. N.; Yano, H.; Nogi, M. Optically transparent composites reinforced with plant fiber-based nanofibers. *Appl. Phys. A* **2005**, *81*, 1109−1112.
(22) Li, T.; Zhu, M.; Yang, Z.; Song, J.; Dai, J.; et al. Wood composite as an energy efficient building material: guided sunlight transmittance and effective thermal insulation. *Adv. Energy Mater.* **2016**, *6*, No. 1601122.
(23) Chen, H.; Baitenov, A.; Li, Y.; Vasileva, E.; Berglund, L. A.; et al. Thickness dependence of optical transmittance of transparent wood: chemical modification effects. *ACS Appl. Mater. Interfaces* **2019**, *11*, 35451−35457.
(24) Chen, C.; Kuang, Y.; Zhu, S.; Burgert, I.; Hu, L.; et al. Structure−property−function relationships of natural and engineered wood. *Nat. Rev. Mater.* **2020**, *5*, 642−666.
(25) Wang, L.; Liu, Y.; Zhan, X.; Luo, D.; Sun, X. Photochromic transparent wood for photo-switchable smart window applications. *J. Mater. Chem. C* **2019**, *7*, 8649−8654.
(26) Gan, W.; Xiao, S.; Gao, L.; Gao, R.; Li, J.; et al. Luminescent and transparent wood composites fabricated by poly(methyl methacrylate) and γ-Fe_2O_3@ YVO_4:Eu^{3+} nanoparticle impregnation. *ACS Sustainable Chem. Eng.* **2017**, *5*, 3855−3862.
(27) Li, Y.; Fu, Q.; Rojas, R.; Min, Y.; Berglund, L.; et al. A new perspective on transparent wood: lignin-retaining transparent wood. *ChemSusChem* **2017**, *10*, 3445−3451.
(28) Samanta, A.; Chen, H.; Samanta, P.; Popov, S.; Berglund, L. A.; et al. Reversible dual-stimuli-responsive chromic transparent wood biocomposites for smart window applications. *ACS Appl. Mater. Interfaces* **2021**, *13*, 3270−3277.
(29) Zhu, M.; Jia, C.; Wang, Y.; Fang, Z.; Dai, J.; Xu, L.; Huang, D.; Wu, J.; Li, Y.; Song, J.; Yao, Y.; Hitz, E.; Wang, Y.; Hu, L. Isotropic paper directly from anisotropic wood: top-down green transparent substrate toward biodegradable electronics. *ACS Appl. Mater. Interfaces* **2018**, *10*, 28566−28571.
(30) Bi, Z.; Li, T.; Su, H.; Ni, Y.; Yan, L. Transparent wood film incorporating carbon dots as encapsulating material for white light-emitting diodes. *ACS Sustainable Chem. Eng.* **2018**, *6*, 9314−9323.
(31) Huang, C.; Lin, W.; Lai, C.; Li, X.; Jin, Y.; Yong, Q. Coupling the post-extraction process to remove residual lignin and alter the recalcitrant structures for improving the enzymatic digestibility of acid-pretreated bamboo residues. *Bioresour. Technol.* **2019**, *285*, No. 121355.
(32) Montanari, C.; Ogawa, Y.; Olsén, P.; Berglund, L. High performance, fully bio-based, and optically transparent wood biocomposites. *Adv. Sci.* **2021**, *8*, No. 2100559.
(33) Sharma, B.; Gatóo, A.; Bock, M.; Ramage, M. Engineered Bamboo for Structural Applications. *Constr. Build. Mater.* **2015**, *81*, 66−73.
(34) Mi, R.; Li, T.; Dalgo, D.; Chen, C.; Hu, L.; et al. A clear, strong, and thermally insulated transparent wood for energy efficient windows. *Adv. Funct. Mater.* **2020**, *30*, No. 1907511.
(35) Zhu, M.; Song, J.; Li, T.; Gong, A.; et al. Highly anisotropic, highly transparent wood composites. *Adv. Mater.* **2016**, *28*, 5181−5187.
(36) Frey, M.; Widner, D.; Segmehl, J.; Casdorff, K.; Keplinger, T.; Burgert, I. Delignified and densified cellulose bulk materials with excellent tensile properties for sustainable engineering. *ACS Appl. Mater. Interfaces* **2018**, *10*, 5030−5037.
(37) Zhou, J.; Wu, Y. Advances in preparation technology and application of transparent wood. *For. Ind.* **2020**, *57*, 17−22.
(38) Gibson, L. The hierarchical structure and mechanics of plant materials. *J. R. Soc. Interface* **2012**, *9*, 2749−2766.
(39) Wang, X.; Shan, S.; Shi, S.; Zhang, Y.; Cai, L.; Smith, L. Optically transparent bamboo with high strength and low thermal conductivity. *ACS Appl. Mater. Interfaces* **2021**, *13*, 1662−1669.
(40) Fu, Q.; Yan, M.; Jungstedt, E.; Yang, X.; Li, Y.; Berglund, L. Transparent plywood as a load-bearing and luminescent biocomposite. *Compos. Sci. Technol.* **2018**, *164*, 296−303.
(41) Li, Y.; Fu, Q.; Yu, S.; Yan, M.; Berglund, L. Optically transparent wood from a nanoporous cellulosic template: combining functional and structural performance. *Biomacromolecules* **2016**, *17*, 1358−1364.
(42) Wu, Y.; Wu, J.; Yang, F.; Tang, C.; Huang, Q. Effect of H_2O_2 leaching treatment on the properties of finished transparent wood. *Polymers* **2019**, *11*, No. 776.
(43) Wu, Y.; Zhou, J.; Huang, Q.; Yang, F.; Wang, J. Study on the properties of partially transparent wood under different delignification processes. *Polymers* **2020**, *12*, No. 661.
(44) Fang, Lu.; Zeng, J.; Liao, X.; Zou, Y.; Shen, J. Tensile shear strength and microscopic characterization of veneer bonding interface with polyethylene film as wood adhesive. *Sci. Adv. Mater.* **2019**, *11*, 1223−1231.
(45) Rana, R.; Langenfeld-Heyser, R.; Finkeldey, R.; Polle, A. FTIR spectroscopy, chemical and histochemical characterisation of wood and lignin of five tropical timber wood species of the family of dipterocarpaceae. *Wood Sci. Technol.* **2010**, *44*, 225−242.
(46) Gierlinger, N.; et al. In situ FT-IR microscopic study on enzymatic treatment of poplar wood cross-sections. *Macromolecules* **2008**, *9*, 2194−2201.
(47) Li, Y.; Yang, X.; Fu, Q.; Rojas, R.; Yan, M.; et al. Towards centimeter thick transparent wood through interface manipulation. *J. Mater. Chem. A* **2018**, *6*, 1094−1101.
(48) Wu, Y.; Wang, Y.; Yang, F. Comparison of multilayer transparent wood and single layer transparent wood with the same thickness. *Front. Mater.* **2021**, *8*, No. 633345.
(49) Fang, L.; Xiong, X.; Wang, X.; Chen, X. Effects of surface modification methods on mechanical and interfacial properties of high-density polyethylene-bonded wood veneer composites. *J. Wood Science* **2017**, *63*, 65−73.
(50) Wu, J.; Wu, Y.; Yang, F.; Tang, C.; Huang, Q.; Zhang, J. Impact of delignification on morphological, optical and mechanical properties of transparent wood. *Composites, Part A* **2019**, *117*, 324−331.
(51) Jia, C.; Tian, L.; Chen, C.; Dai, J.; Kierzewski, I.; Song, J.; Li, Y.; Yang, C.; Wang, C.; Hu, L. Scalable, anisotropic transparent paper directly from wood for light management in solar cells. *Nano Energy* **2017**, *36*, 366−373.
(52) Huang, C.; Tang, S.; Zhang, W.; Tao, Y.; Lai, C.; Xi, L.; Yong, Q. Unveiling the structural properties of lignin-carbohydrate complexes in bamboo residues and its functionality as antioxidants and immunostimulants. *ACS Sustainable Chem. Eng.* **2018**, *6*, 12522−12531.
(53) Zhang, L.; Wang, A.; Zhu, T.; Chen, Z.; Wu, Y.; Gao, Y. Transparent wood composites fabricated by impregnation of epoxy resin and w-doped VO_2 nanoparticles for application in energy-saving windows. *ACS Appl. Mater. Interfaces* **2020**, *12*, 34777−34783.

https://doi.org/10.1021/acsomega.1c05014
ACS Omega 2021, 6, 33747−33756